COMPARISONS OF LIDAR, ACOUSTIC AND TRAWL DATA ON TWO SCALES IN THE NORTHEAST PACIFIC OCEAN

JAMES H. CHURNSIDE
NOAA Earth System Research Laboratory
325 Broadway
Boulder, Colorado 80305

DAVID A. DEMER
NOAA Southwest Fisheries Science Center
8604 La Jolla Shores Drive
La Jolla, California 92037

DAVID GRIFFITH
NOAA Southwest Fisheries Science Center
8604 La Jolla Shores Drive
La Jolla, California 92037

ROBERT L. EMMETT
NOAA Northwest Fisheries Science Center
2030 S. Marine Science Drive
Newport, Oregon 97365

RICHARD D. BRODEUR
NOAA Northwest Fisheries Science Center
2030 S. Marine Science Drive
Newport, Oregon 97365

ABSTRACT

We compared measurements of integrated optical volume backscattering coefficients $\beta(\pi)$ with integrated acoustic volume backscattering coefficients (s_v) and surface-trawl catches over a large-scale (roughly 300 km by 450 km) region, and a small-scale (roughly 50 km by 50 km) region off the coasts of Oregon and Washington. In both cases, the data were significantly correlated. For the large-scale data, the correlation was better (R = 0.78) when the lidar data were collected at night compared to during the day, probably because the fish ascend into the near-surface layer at night. For the small-scale survey, lidar data were only collected at night, and the correlation was higher (R = 0.98). With the large-scale data set, we performed a simulation of an adaptive sampling technique that would use the airborne lidar to direct the acoustic survey. This could significantly reduce ship time with only a modest decrease in the quality of the results.

INTRODUCTION

Pacific sardine (*Sardinops sagax*) is currently one of the dominant pelagic fish species in the northern California Current and is an important ecological component of this ecosystem (Emmett et al. 2005). Since sardines are commercially important, accurate stock assessments are important for successful management. They are presently assessed by a combination of acoustic/trawl surveys and egg production estimates (Emmett et al. 2005; Hill et al. 2006; Cutter and Demer 2008). Their abundance fluctuates greatly over a vast region of the California Current, so comprehensive ship surveys are expensive.

However, sardines often form near-surface schools that have patchy distributions over large areas, and this behavior suggests that aerial survey data could aid assessments and thus those responsible for management.

Detection of fish schools by airborne lidar was demonstrated originally by Squire and Krumbolts (1981). More recently, comparisons of lidar and echosounder measurements of capelin and herring (Brown et al. 2002), mullet and baitfish (Churnside et al. 2003), zooplankton (Churnside and Thorne 2005), and epipelagic juvenile fish (Carrera et al. 2006) have demonstrated good agreement when the measurements were made within a few days and both lidar and echosounder data were appropriately filtered to remove unwanted signals.

In this study, the results of aerial lidar surveys were compared with those from a large-scale echosounder survey off the coast of Oregon and Washington and a small-scale trawl survey near the mouth of the Columbia River. Various algorithms were applied to the lidar data, and their correspondence with the echosounder and trawl results investigated. The results were similar to those of previous studies (Carrera et al. 2006; Churnside et al. 2009a), which found median filtering and thresholding of lidar data to produce good correlation with ship survey results. The data from the large-scale survey were also used to retrospectively investigate how the lidar survey might have been used to direct an adaptive survey with the ship.

METHODS

The study area for the large-scale survey (fig. 1) extended from near the shore out to almost 128°W and from 44° to 48°N. The FV *Frosti* collected acoustic data along constant-latitude lines during the day, and oceanographic profiles and surface trawls at night. The National Oceanic and Atmospheric Administration (NOAA) Fish Lidar was flown out and back along the same transect line during the afternoon of the acoustic survey and again starting at least one hour after sunset that same evening. The five transect lines were flown on July 9 (44°N), 10 (45°N), 11 (46°N), 13 (47°N), and 16 (48°N) in 2003.

The echosounder (Simrad ES60) was configured with a 38 kHz split-beam transducer (Simrad ES38-B; 7° beam width), hull-mounted at a nominal depth of four meters. Volume backscattering strengths (S_v) less than -55 dB (re 1 m^{-1}) or greater than -25 dB were removed. The remaining volume backscattering coefficients (s_v) (per m) were integrated from depth d = 7 m (three meters below the transducer) to d = 254 m, and averaged over 0.5°-longitude intervals along each transect, resulting in 39 area-backscattering coefficients (s_a)(m^2/nmi^2).

The NOAA Fish Lidar (Churnside et al. 2001; Churnside 2008) transmitted a short (12 ns), intense (120 mJ)

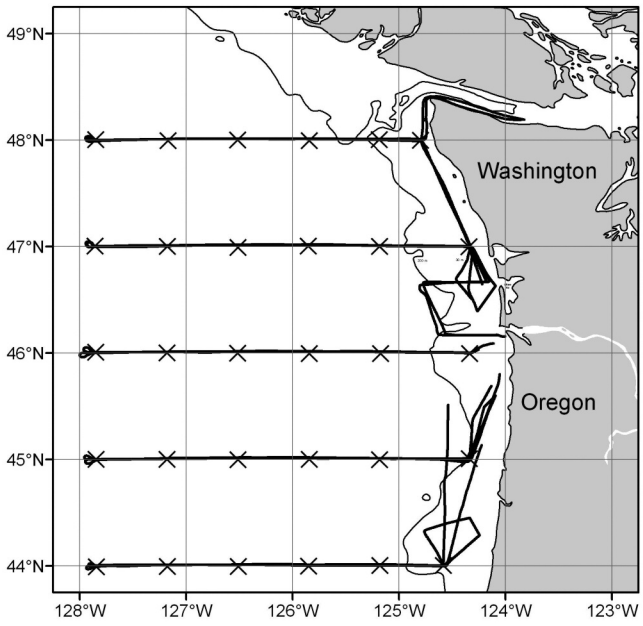

Figure 1. Chart of large-area survey region showing all flight tracks (heavy black lines) and oceanographic sampling stations (X) off the coast of Oregon and Washington in July 2003. The light black line is the 200 m isobath. Acoustic data were collected along the lines defined by the flight tracks and oceanographic stations.

pulse of green (532 nm) laser light that was diverged to produce a 5 m diameter spot on the sea surface. The receiver used a 17 cm diameter telescope to collect the backscattered light onto a photomultiplier tube. A polarizing filter rejected light in the same plane as the laser beam, while allowing light depolarized by scatterers in the air and the ocean to pass through. The detector output was log-amplified and digitized at 10^9 samples per second, which corresponds to one volume backscattering coefficient ($\beta(\pi)$) measurement every 11 cm through the upper water column. The aircraft flew at an altitude of 300 m and at a speed of 90 m/s. At this speed, and with a pulse-repetition frequency of 30 Hz, the laser pulses were separated horizontally by 3 m.

The first lidar data-processing filter, denoted "linear," was based on the assumption that background scattering within the water column was constant with depth for each pulse. This implies that the logarithm of the background-$\beta(\pi)$ profile is linear. The function:

$$\beta(\pi) = a(\exp(2\alpha d)) + b,$$

where a is a proportionality constant, α is the attenuation coefficient, and b is a constant offset, was estimated from the $\beta(\pi)$ between a depth of 2 m and at the depth of the lower limit, where the signal initially drops below 10 standard deviations of the electronic noise of the receiver. Measurements of $\beta(\pi)$ from the top 2 m were occasionally contaminated by breaking waves and bubbles; those from depths below the lower limit were affected by noise. The fitted function was used to estimate $\beta(\pi)$ and α for each pulse. Where $\beta(\pi)$ was greater than the background-$\beta(\pi)$ by a factor greater than a threshold T, it was assumed to be from fish, and it was included in the integration. The integration in this case was done over all depths between the endpoints of the fit and averaged over 0.5°-longitude segments of the flight track (bins) to match the s_a bins. Two values of integrated $\beta(\pi)$ were produced for each bin from measurements from each flight; one going west and the other east over the same trackline. These two values were averaged.

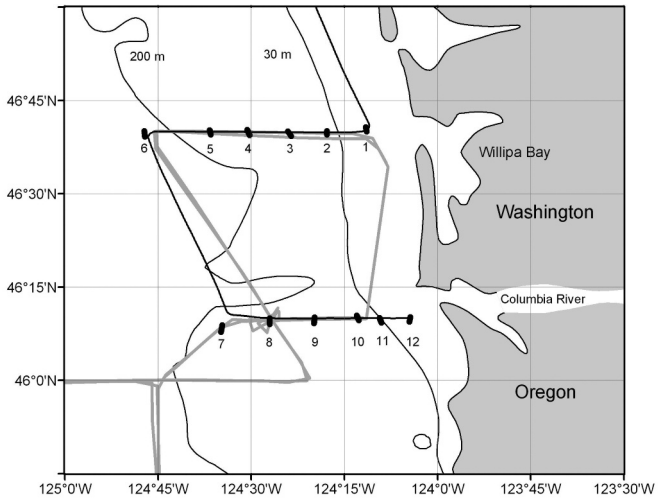

Figure 2. Chart of small-area survey region showing trawl lines of 12 trawl stations and flight tracks for the nights of 16 July (black) and 17 July (grey) 2003.

The second lidar data-processing filter, denoted "median," was based on the assumption that the background $\beta(\pi)$ at any depth was uniform along some segment of the flight track. The background $\beta(\pi)$ and α for each segment along the flight track were estimated from the median profile of the pulses within that segment, so the segment length represents the length of the median filter. The application of a threshold and the integration were done as in the linear filter.

The study area for the small-scale survey (fig. 2) was defined by the Northwest Fisheries Science Center's Predator Survey, which is a surface trawl survey of pelagic fish (Emmett et al. 2005). This survey consists of 12 trawls along two east-west transects, one off the mouth of the Columbia River and the other to the north. The trawls were made on the nights of 16 (Stations 1–6) and 17 (Stations 7–12) July 2003. Two flights were made on the same nights along the tracks shown in the Figure 2 at a speed of about 80 m/s.

Fish were sampled at night using a Nordic 264 rope trawl (NET Systems[1], Bainbridge Island, Washington)

[1]Reference to trade name does not mean endorsement by NOAA, National Marine Fisheries Service.

fished directly astern the vessel at the surface. The trawl has an effective fishing mouth of 12 m deep and 28 m wide (336 m^2) as identified during an early cruise (June 2000) using net mensuration equipment (Emmett et al. 2004). The mouth was spread apart by a pair of 3.0 m foam-filled trawl doors. The trawl was towed with about 300 m of warp for 30 min at 1.5 m/sec. To fish the trawl at the surface, a cluster of two meshed A-4 Polyform buoys were tethered to each wing tip and two single A-4 Polyform floats were clipped on either side of the center of the headrope. Mesh sizes ranged from 162.6 cm in the throat of the trawl near the jib lines to 8.9 cm in the cod end. To maintain catches of small fish and squid, a 6.1 m long, 0.8 cm mesh knotless liner was sewn into the codend.

Fish captured in trawls were separated by species, counted, and fork length (FL) (mm) was measured for up to 50 of each species. However, for very large catches, a subsample was measured, counted, and weighed; the remaining fish of each species were weighed collectively. The total number of each species was then estimated using the known number of fish per kg. Density was calculated by multiplying the number of each species in a haul by the volume of water the net fished, and standardized to number per 10^6 m^3. The volume of water fished was calculated from the trawled distance multiplied by the effective net-mouth area (336 m^2).

For comparison with net catches, the lidar data were processed in the same way as for the large-scale survey, except for the size of the bins used for averaging. The 0.5°-longitude bins used for the large-scale survey were far too large for the small-scale survey, so a bin was defined for each trawl station instead. For Stations 2–5 and 8–11, the bin extended from the midpoint of the trawl to the stations before and after the trawl. The bins at the ends on the two lines included measurements of $\beta(\pi)$ from within a circle with a radius equal to half the distance to the nearest bin.

For each combination of lidar data and acoustic or catch data, the Pearson sample correlation coefficient R was calculated. The significance p of each correlation was estimated using Student's t test.

RESULTS

For the large-scale survey, the correlation coefficient R for each combination of parameters is presented in Table 1. The acoustic data were compared separately with the daytime survey and with the night-time survey. The statistical significance of R increases with increasing R, so that any value of $R > 0.4$ has a significance $p < 0.01$. For the daytime lidar data, the correlation is only significant ($p < 0.01$) using a median filter with a threshold of one. The correlation for these cases decreases with increasing filter length. For the night-time lidar data, the situation is somewhat different. The correlation using a median filter with a threshold of one is nearly 0.73, with no dependence on the length of the filter. This correlation is significantly greater than during the daytime.

TABLE 1
Correlation coefficient (R) between echosounder and lidar data for the large-scale survey, with daytime and night-time lidar data considered separately.

Filter	Length (m)	Threshold	R (daytime)	R (night-time)
linear	—	1	0.38	0.65
linear	—	2	0.03	0.56
linear	—	3	−0.04	0.15
median	75	1	0.52	0.73
median	75	2	0.20	0.32
median	75	3	0.21	0.12
median	150	1	0.49	0.72
median	150	2	0.27	0.36
median	150	3	0.27	0.22
median	300	1	0.47	0.74
median	300	2	0.30	0.48
median	300	3	0.29	0.33
median	750	1	0.45	0.73
median	750	2	0.32	0.77
median	750	3	0.29	0.69
median	1500	1	0.44	0.74
median	1500	2	0.33	0.78
median	1500	3	0.32	0.52

TABLE 2
Density (number of fish per 10^6 m^3) for each haul by species, and total catch of all species from the Predator Survey in July 2003.

Haul Number	Eulachon	Northern Anchovy	Pacific Herring	Pacific Sardine	Total
1	73.22	79.68	4.31	0	157.20
2	0	1502.59	3143.19	64293.50	68939.27
3	0	43.04	557.71	147.85	748.60
4	0	10.79	113.33	0	124.12
5	0	0	105.15	2.19	107.34
6	0	0	0	0	0
7	0	2.82	227.20	0	230.02
8	0	227.72	13.49	462.18	703.40
9	0	60.20	6.69	6739.34	6806.23
10	44.92	8.17	57.17	22.46	132.71
11	23.69	17.77	1.97	0	43.44
12	0	12.07	60.36	0	72.44

The catch results for the small-scale survey are presented in Table 2. It is important to note that 88% of the total density was recorded at Station 2. Also, 92% of the catch was sardine.

The density of total fish was compared with the measured $\beta(\pi)$ to investigate the effects of filter type, filter length for the median filter, and threshold level. The significant ($p < 0.01$) correlations are presented in Figure 3. The results in the Columbia River plume show very high correlations for the smaller filter lengths and the highest thresholds that produced meaningful results.

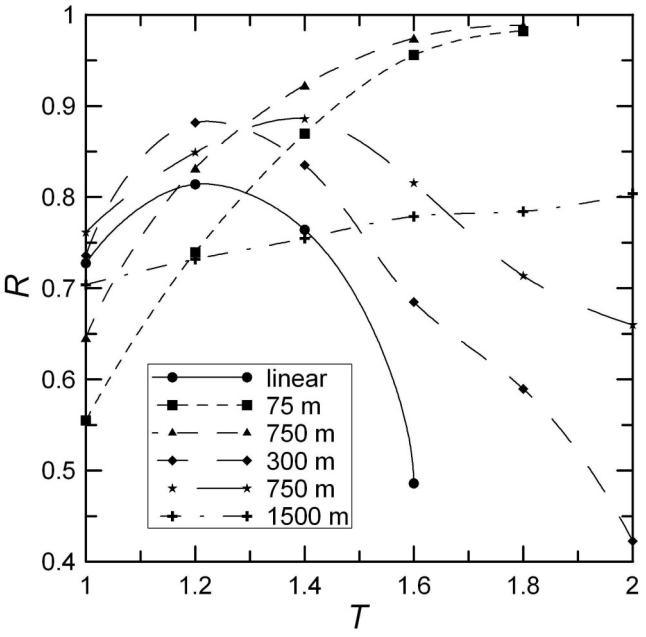

Figure 3. Correlation coefficient *R* between density of all fish in the surface trawls and the light backscatter as a function of threshold level *T* for the linear filter and the median filter with varying filter length for 2003 small-scale survey.

Increasing the threshold beyond $T = 1.8$ removed all of the $\beta(\pi)$ from most of the lidar averaging bins. Most of this correlation is due to the one very large value in both the density and the lidar backscatter. However, this is not the only correspondence. For example, there is a high correlation ($R = 0.996$, $p = 10^{-8}$) between the density of northern anchovy in the catches and the lidar signal with a filter length of 75 m and a threshold value of 1.8. Anchovy made up a small fraction of the total catch (2.5%), but were strongly associated with sardines ($R = 0.995$, $p = 10^{-6}$).

DISCUSSION

There are several interesting patterns of correlation in the large-scale survey results. These are very different in the daytime and night-time lidar data. The lidar data suggest that more of the fish that are in the depth range of the echosounder during the day ascend closer to the surface at night. These patterns are consistent with observations of sardine migrating closer to the surface and forming larger, less dense aggregations at night (Krutzikowsky and Emmett 2005; Cutter and Demer 2008). Previous computer simulations with another pelagic species that migrates vertically (northern anchovy, *Engraulis mordax*) confirm that night-time surveys will be less biased due to the fraction of the population which resides below the lidar-observation depth during the day (Lo et al. 2000).

Since higher thresholds remove contributions from weaker scatterers, it is clear that the acoustic targets are not strong lidar scatterers. Also, the median filter will remove contributions from objects larger than half of the filter length. The schools observed with the echosounder are generally smaller than about 40 m during the daytime. When the filter length is greater than 80 m, the lidar can detect objects larger than 40 m that would not be seen by the echosounder. These large objects could be plankton layers, which were visually detected in the lidar data (Churnside and Donaghay 2009). That there is no dependence on filter length suggests that the contribution from larger objects like plankton layers is negligible. For lower filter lengths (≤300 m), the correlation decreases as the threshold increases. This implies that a significant fraction of the $\beta(\pi)$ from fish is less than the threshold value. For the greater filter lengths, the correlation at $T = 2$ is slightly greater than that at $T = 1$. The implication is that there is a greater range of school size at night.

An adaptive survey was simulated using the night-time lidar data with a median filter of length 1500 m. The ship went more than 200 nm offshore on all of the transects, but most of the fish were much closer. If it were known a priori that there were no fish at the west end of the transects, the ship could have covered a smaller area with insignificant degradation of the results. For example, assuming that the ship would be sent to all regions where the $\beta(\pi)$ was above 1% of its maximum value, and using a $T = 1$, the ship would only need to survey 64% of the original area, but would still sample 89% of the acoustic backscatter from the full survey. This suggests that ship costs can be significantly reduced with little reduction in the quality of the survey. Increasing the threshold to $T = 2$ eliminates less dense aggregations of fish. In this case, with a focus on the denser schools, the ship time is reduced to 28% of the original, but the simulated survey still samples 70% of the acoustic backscatter. Specific cost/benefit analyses need to be performed for future surveys, but the unmistakable conclusion is that survey costs could be reduced using adaptive survey techniques based on the combination of data from airborne lidar and ship-based echosounders.

Remote sensing of pelagic nekton, combining aerial imagery and lidar with ship-based echosounder and direct sampling can provide a more accurate assessment at a lower cost than direct sampling alone (Churnside et al. 2009b). Lidars and echosounders provide complementary information but sample different parts of the water column. Lidar samples to the surface, but can only observe 10–50 m into the water column, depending on water clarity. An echosounder can sample to greater depths than a lidar, and either measures the fraction of the population below the lidar observation depth, or ensures that the lidar is sampling the entire population, depending on conditions.

Lidar can overcome some of the limitations that acoustical techniques have in detecting very shallow fish.

Lidar can detect fish at the surface, above the depth of a hull-mounted transducer and its associated near-field dead zone (Holliday and Larsen 1979). In addition, fish do not avoid aircraft, as they sometimes do for surface vessels (Fréon and Misund 1999). Moreover, lidar surveys can sample large areas quickly, providing synoptic views, but cannot stop to sample fish aggregations to get more detailed information. An echosounder can be used to direct scientific fishing, but may not be able to cover a large area fast enough to prevent aliasing of temporal scales into spatial scales. Thus, when possible, a combination of the two remote-sensing techniques, with complementary trawling to provide identification of the targets, could be used to provide rapid and reliable assessments of epipelagic species (Gauldie et al. 1996; Santos 2000; Churnside et al. 2009b).

ACKNOWLEDGMENTS

This work was partially supported by the National Ocean Partnership Program and the NOAA Office of Ocean Exploration. Funding for the trawl collections comes from the Bonneville Power Administration and the NOAA Fisheries Northwest Fisheries Science Center.

LITERATURE CITED

Brown, E. D., J. H. Churnside, R. L. Collins, T. Veenstra, J. J. Wilson, and K. Abnett. 2002. Remote sensing of capelin and other biological features in the North Pacific using lidar and video technology. ICES J. Mar. Sci. 59:1120–1130.

Carrera, P., J. H. Churnside, G. Boyra, V. Marques, C. Scalabrin, and A. Uriarte. 2006. Comparison of airborne lidar with echosounders: a case study in the coastal Atlantic waters of southern Europe. ICES J. Mar. Sci. 63:1736–1750.

Churnside, J. H. 2008. Polarization effects on oceanographic lidar. Opt. Exp. 16:1196–1207.

Churnside, J. H. and R. E. Thorne. 2005. Comparison of airborne lidar measurements with 420 kHz echo-sounder measurements of zooplankton. Appl. Opt. 44: 5504–5511.

Churnside, J. H. and P. L. Donaghay. 2009. Thin scattering layers observed by airborne lidar. ICES J. Mar. Sci. 66:778–789.

Churnside, J. H., J. J. Wilson, and V. V. Tatarskii. 2001. Airborne lidar for fisheries applications. Opt. Engin. 40:406–414.

Churnside, J. H., D. A. Demer, and B. Mahmoudi. 2003. A comparison of lidar and echosounder measurements of fish schools in the Gulf of Mexico. ICES J. Mar. Sci. 60:147–154.

Churnside, J. H., E. Tenningen, and J. J. Wilson. 2009a. Comparison of data-processing algorithms for fish lidar detection of mackerel in the Norwegian Sea. ICES J. Mar. Sci. 66:1023–1028.

Churnside, J., R. Brodeur, J. Horne, P. Adam, K. Benoit-Bird, D. C. Reese, A. Kaltenberg, and E. Brown. 2009b. Combining techniques for remotely assessing pelagic nekton: getting the whole picture. *In* The Future of Fisheries Science in North America, R. Beamish and B. Rothschild, eds. Springer, Berlin, pp. 345–356.

Cutter, G. R., Jr. and D. A. Demer. (Co-Editors). 2008. California Current Ecosystem Survey 2006, NOAA-TM-NMFS-SWFSC-415.

Emmett, R. L., R. D. Brodeur, and P. M. Orton. 2004. The vertical distribution of juvenile salmon (*Oncorhynchus* spp.) and associated fishes in the Columbia River plume. Fish. Oceanog. 13:392–402.

Emmett, R. L., R. D. Brodeur, T. W. Miller, S. S. Pool, G. K. Krutzikowsky, P. J. Bentley, and J. McCrae. 2005. Pacific sardine (*Sardinops sagax*) abundance, distribution, and ecological relationships in the Pacific Northwest. Calif. Coop. Oceanic Fish. Invest. Rep. 46:122–143.

Fréon, P. and O. A. Misund. 1999. Dynamics of Pelagic Fish Distribution and Behaviour: Effects on Fisheries and Stock Assessment. Fishing News Books, Oxford, UK 348 p.

Gauldie, R. W., S. K. Sharma, and C. E. Helsley. 1996. LIDAR applications to fisheries monitoring problems. Can. J. Fish. Aquat. Sci. 53:1459–1468.

Hill, K. T., N. C. H. Lo, B. J. Macewicz, and R. Felix-Uraga. 2006. Assessment of the Pacific sardine (*Sardinops sagax caerulea*) population for U.S. management in 2007. U.S. Dep. Commerce, NOAA Tech. Memo. NOAA-TM-NMFS-SWFSC-396, 105 pp.

Holliday, D. V., and H. L. Larson. 1979. Thickness and depth distributions of some epipelagic fish schools off southern California. Fish. Bull. 77:489–594.

Krutzikowsky, G. K., and R. L. Emmett. 2005. Diel differences in surface trawl catches off Oregon and Washington. Fish. Res. 71:365–371.

Lo, N. C. H., J. R. Hunter, and J. H. Churnside. 2000. Modeling statistical performance of an airborne lidar survey system for anchovy. Fish. Bull. 98:264–282.

Santos, A. M. P. 2000. Fisheries oceanography using satellite and airborne remote sensing methods: a review. Fish. Res. 49:1–20.

Squire, J. L. and H. Krumboltz. 1981. Profiling pelagic fish schools using airborne optical lasers and other remote sensing techniques. Mar. Tech. Soc. J. 15:27–31.